An Overview of Polymersomes and Their Shape Transformation into Stomatocytes for Use as Nanocarriers and Nanoreactors

SOFIA C. SANTOS[1], JORGE M. SANTOS[2]
[1]Instituto de Ciências Biomédicas Abel Salazar, Universidade do Porto,
Porto,
PORTUGAL

[2]Instituto Superior de Engenharia do Porto, Politécnico do Porto,
Porto,
PORTUGAL

Abstract: - Polymersomes are self-assembled vesicles from amphiphilic block copolymers, bi-layered with a spherical morphology, that have very interesting characteristics. They have good physical and chemical stability; several changes can be made to the surface, and they can also encapsulate a wide range of molecules with different affinities to water. For these reasons, polymersomes and the different non-spherical shapes that can be obtained from them, have been the target of intense research with the ambition of creating new tools and structures within the scope of biomimicry and nanomedicine. One of the main challenges is to establish protocols for changing the shape of the polymersomes in a controlled way, to expand the number of possible applications. In this work, an overview of the most important methodologies for shape transformation is presented, along with some examples of stomatocyte applications.

Key-Words: - Polymersomes, Stomatocytes, Shape Transformation, Nanocarriers, Nanoreactors, Copolymers, Self-Assembly.

Received: May 21, 2024. Revised: December 23, 2024. Accepted: January 18, 2025. Published: May 9, 2025.

1 Introduction

Cells have delineated structures containing a set of enzymes that perform specific functions. Forming structures that resemble the cell, or its organelles has been for a long time a matter of deep investigation. Achieving a biomembrane-like bilayer structure for the first time in 1977, [1] encouraged ongoing investigations into the subject. Since then, various vesicles and cellular-like structures have been developed with well-established protocols, [2], [3], [4].

It was previously known that liposomes can transform their shape as a response to environmental changes, namely by fluctuations in the osmotic conditions, composition of the lipids or even temperature, [5], [6].

The highly flexible membrane of liposomes does not allow for easy capture of transient morphologies since the transitions between different shapes occur in very short timescales. In comparison to liposomes, polymeric vesicles allow one to stop at a certain morphology and not only obtain interesting, but transient morphologies, [7].

Polymersomes are composed of building blocks with molecular weights much higher than those of the typical phospholipids present in natural membranes and liposomes. This characteristic kinetically hampers polymer chain rearrangements and chain exchanges between polymersomes and even with free polymers in solution. This means that polymersomes are kinetically trapped structures and tend to be spherical to minimize interfacial tension and stay in the most energetically favorable shape.

To obtain more biologically relevant shapes from polymersomes, one must play with the glass transition temperature (T_g) of the building blocks, the chain size or molecular weight, the anisotropy between both leaflets of the membrane, stimuli-responsive block copolymers, and preparation conditions.

Polymersomes and subsequent non-spherical shapes are promising structures for newer and better ways to encapsulate and compartmentalize cargo and have potential applications in many areas: drug delivery systems, imaging, nanoreactors and nanomotors, and mimes of the living systems and organelles, [8].

2 Principles of Polymersome Formation

The building blocks, amphiphile block copolymers (possessing both hydrophilic and hydrophobic domains), especially diblock ones, are made through living polymerization techniques [9], such as Atom Transfer free Radical Polymerization (ATRP) [10], Reversible Addition-Fragmentation chain-Transfer Polymerization (RAFT) [11], Ring-opening Metathesis Polymerization and Ring-opening Polymerization (ROP) [12].

The classic mathematical descriptions would roughly estimate that for hydrophilic fractions (hydrophilic portion to total mass) between 0.25 and 0.45 the self-assembly process would yield Polymersomes and when $f_{\text{hydrophilic}}$>50, worm-like micelles would be obtained, [8]. These predictions come from the relationship between hydrophilic fraction and the curvature of the hydrophobic-hydrophilic interface, and the packing parameter $p = \frac{v}{a*l}$ (v = volume of the hydrophobic part, a = interfacial area per molecule and l = chain length of the hydrophobic part, normalized to the interface), [13]. However, these mathematical predictions for the self-assembly process of small molecules surfactants do not explain all self-assembly behaviors of block copolymers.

Mechanism I, as outlined in the literature, is widely accepted as the primary model for the formation of polymersomes. Adapted from [14], [15], this self-assembly process consists of two main steps: first, the self-assembly of bilayer sheets; and second, the bending and fusion of these sheets into spherical vesicles (Figure 1a). The bending and closure occur due to an increase in edge energy resulting from the solvation of hydrophobic components along the bilayer's edges. When the edge energy surpasses the bending energy—the energy required to bend the bilayers—the bilayer naturally folds in on itself, reducing free energy and forming spherical particles.

Another mechanism is presented where, instead of the formation of bilayer sheets, there is a formation of micelles that gradually increase their volume with the entry of solvent into the core and progressively grow to form vesicles (Figure 1b). For now, due to all the different block copolymer preparations that can be made, it is difficult to predict and explain all self-assembly pathways for the formation of polymersomes.

3 Methodologies for Polymersome Formation

The techniques to prepare polymersomes are mainly categorized into two different groups: solvent-switching techniques and polymer rehydration or solvent-free techniques.

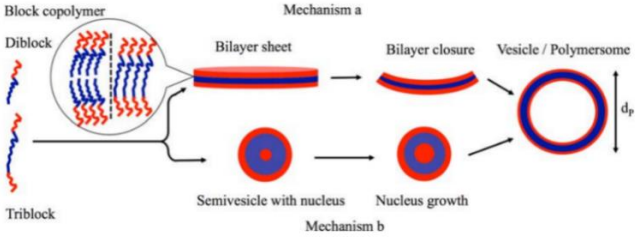

Fig. 1: A scheme that demonstrates different mechanisms for the self-assembly of polymersomes. a) two-step mechanism I. b) mechanism based on the growth of micelles. Adapted from [16]

3.1 Solvent-switching/Co-solvent

The amphiphilic block copolymers are firstly dissolved in an organic solvent, that is chosen according to the blocks, followed by hydration of the solution (either by the slow addition of water to the organic polymer solution or by the injection of the organic solution into water). The hydrophobic portion, being insoluble upon hydration, forces the self-assembly of the copolymers into polymersomes, due to an increase of interfacial tension between the hydrophobic blocks and water. Organic solvents, such as tetrahydrofuran (THF) [17], chloroform, dioxane and N,N-dimethylformamide (DMF) are the most commonly used, [18].

3.2 Solvent-free

The most common technique within this group is *film rehydration*, where one starts by dissolving the block copolymers in a suitable organic solvent, which is then (vacuum) dried/evaporated, leaving a thin film of amphiphile, [19], [20]. Subsequent film hydration yields vesicles (and other self-assembled aggregates).

pH switch is another technique where the block copolymers, which are pH sensitive self-assemble or dissociate after changes in pH, [21].

Electroformation is also useful for the formation of giant polymersomes, [22], [23].

Novel methodologies aim to reduce some disadvantages of the traditional methods such as the use of organic solvents which are usually not biocompatible and the fact that not always one can

get desired sizes, good size distributions and ideal concentrations. Dual asymmetry centrifugation (DAC) presents a new method that requires no after-processing of the polymersomes to control size and yield concentrated samples, [24].

4 Polymersome Controlled Shape Transformation

Polymersome morphology can be controlled by the amphiphilic block copolymers and subsequently re-shaped through chemical or physical stimuli, [25].
In the following subsections, different established methodologies are presented according to categories suggested in [26].

4.1 Osmotically Induced

The osmotically induced methodologies can be subdivided into the following:

4.1.1 Direct Dialysis

The use of osmotic pressure to drive the shape change of the polymersomes into stomatocytes in a controlled manner was initially performed in [27]. The pillar for this methodology lies in the fact that the osmotic equilibrium of the polymersomes in solution only exists at the precise moment they self-assemble. Pushing the polymersomes out of osmotic equilibrium can be done by introducing a variable that changes the composition of the solvent, forcing them to reach another state of equilibrium which would ideally reflect in any desired new morphology, [17].

The authors take advantage of the phase behavior of the glassy hydrophobic polymeric segment utilized (T_g = 100ºC), giving them the ability to capture different shapes of polymersomes by kinetically controlling them.

Polymersomes from poly(ethylene glycol)-*block*-poly(styrene) (PEG_{45}-*b*-$PS_{176/292}$) are first generated by the addition of water to a solution of polymer in organic solvents – THF/dioxane (1:1 v/v) – **solvent-switching method**

The addition of water is done dropwise, recurring to a syringe pump, forcing the polymer to self-assemble due to the hydrophobicity of PS in PEG-PS. Polymersomes (100-500nm) form and a cloudy suspension is observed.

To induce shape transformation, the mixture is transferred to a dialysis bag and dialyzed against water (Figure 2). This will cause a quick expulsion of solvent molecules held within the core of the polymersomes to maintain osmotic equilibrium (Figure 3). The rate of outward transport of THF and dioxane molecules across the swollen polymersome membrane is higher than the entrance of water molecules (this can be explained by the comparison of the Hildebrand solubility parameters of the solvents (δ =18.6 [MPa]1/2) for THF and (δ = 20.5 [MPa]1/2 for dioxane and water (δ = 48 [MPa]1/2) with the parameter of homo-PS (δ = 16.6-20.2 [MPa]1/2), [28].

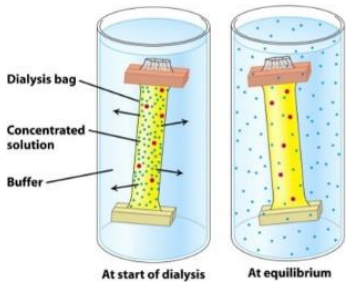

Fig. 2: Schematics of the dialysis process

The membrane will gradually transform into its rigid and glassy state and lose its permeability as the solvent molecules diffuse out of the core. The entrance of water molecules in the inner compartment and replacement of the fast-outward diffusing organic molecules is, therefore, progressively hindered, decreasing the volume of the inner compartment. Due to the negative osmotic pressure generated, the membrane is forced to fold inwards, leading to the formation of stomatocytes. The authors propose that the change in shape comes from the decrease in the volume of the inner compartment, instead of the generation of structural asymmetry in the membrane structure which translates into changes in the surface area.

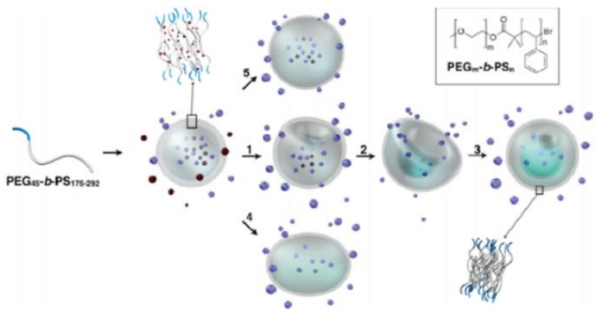

Fig. 3: Shape transformation pathway of the above-described method (1,2,3). The red dots correspond to organic solvent molecules and the blue dots correspond to water molecules. (5) shows the result of rapidly quenched polymersomes with water. The shape change of polymersomes can also go through the prolate pathway (4), depending on methodology and block copolymer modification. Adapted from [27].

Instantly adding a significant amount of water to the polymersome suspension or provoking a fast decrease in temperature, will rapidly freeze the morphology as a result of a rapid quenching of the hydrophobic domain, that vitrifies, due to its high T_g. This sudden cooling provides enough physical strength such that the thermodynamically favored spherical morphology is kept. Indeed, the phase behavior of the hydrophobic domain (from a solvent-swollen fluidic state to a glassy rigid state) allows the retention of the morphology after shape transformation. Contrarily, with recurrence to a plasticizing solvent, the T_g can be lowered to or below ambient conditions so that, even at room temperature, there is improved chain mobility and dynamicity, and shape transformations can occur. By raising the T_g back up with the removal of the plasticizing solvent or the addition of non-solvent, new non-spherical morphologies can be kinetically trapped.

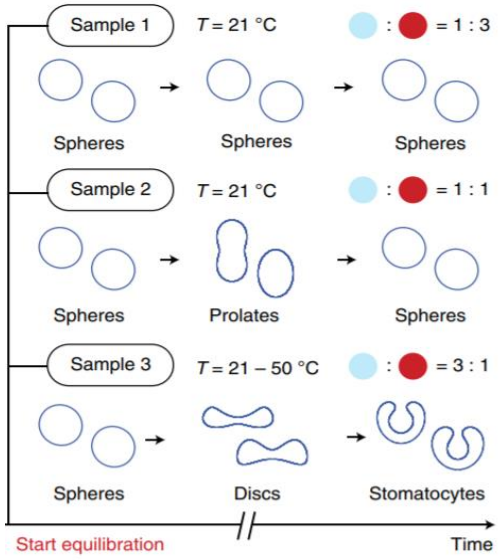

Fig. 4: The behavior that polymersomes have right after self-assembly, in response to the amount of water present. The water added after the spontaneous self-assembly into polymersomes changes the solvent composition of the surroundings, starting a new seek for osmotic equilibrium. (Sample 1) 1mL of water is added *via* a syringe pump to a 3mL polymer solution in THF:dioxane (3:2, v:v). (Sample 2) 2mL of water is added *via* syringe pump to a 2mL polymer solution in THF:dioxane (3:2, v:v). (Sample 3) 3mL of water is added *via* syringe pump to a 1mL polymer solution in THF:dioxane (3:2, v:v). Adapted from [17]

It should be noted that dialysis against the water of the polymersome suspension can generate other morphologies rather than just stomatocytes or not lead to a change in shape at all. Authors better explain that the extent of the osmotic pressure generated after the self-assembly into polymersomes is related to the amount of the organic solvents that are used and the volume of water that is added, [17] (Figure 4).

Analyzing and comparing more recent reports [29], [30] where the organic solvent is removed from polymersome suspension by dialysis against water for at least 24 hours, yielding polymersomes with glassy membranes, instead of stomatocytes, it is established that the initial water volume in the ratio water/organic solvents present in the polymersome suspension influences the generation of stomatocytes and even more the final shape.

Modified literature procedures resorting to direct dialysis to either prepare stomatocytes [27] or polymersomes [31] are schematically represented in Figure 5.

PEG_{45}-b-PS_{292} (20 mg) is dissolved in THF:dioxane (2mL, 60:40, v:v).	PEG_{45}-b-PS_{182} (10 mg) is dissolved in THF:dioxane (1mL, 60:40, v:v).
2mL of pure water is added *via* syringe pump (1mL/h).	3mL of pure water is added *via* syringe pump (1mL/h).
The final suspension is transferred to a dialysis membrane and the vesicles dialyzed against ultrapure water for 24h.	The final suspension is transferred to a dialysis membrane and the vesicles dialyzed against ultrapure water for 24h.
This yielded *stomatocytes*	This yielded *polymersomes*

Fig. 5: Direct dialysis procedures for the preparation of stomatocytes (left) or polymersomes (right) through dialysis against the same amount of water

Nature of shape transformation

Before presenting the methodologies in the next subsections, a description of the nature of shape transformation must be given, for better understanding.

In shape transformations, bending energy needs to be considered, since studies show it strongly influences the pathway of shape change, [32]. The bending energy (*Eb*) of the membrane is defined as,

$$E_b = \frac{k}{2}\oint(2C - C_0)^2 dA \quad (1)$$

where k is the bending rigidity of the membrane, C is the mean surface curvature, C_0 is the spontaneous curvature and A is the surface area.

As the equation shows, E_b is a function of k, C and C_0. Bending rigidity (k) is determined by the membrane's chemical properties (length and composition of the building blocks) and by other environmental factors such as solvent and temperature. Mean surface curvature (C) represents the degree of curvature at different points along the membrane. Finally, spontaneous curvature (C_0) reflects any asymmetry in copolymer conformation between the two (inner and outer) leaflets in the bilayer membrane and therefore this parameter is sensitive to the membrane's microenvironment on both sides.

From the presented above, it is clear that the osmotic pressure strategy for shape transformation deals with a complex relationship between bending energy and osmotic energy. During dialysis of polymersomes against water, depending on the amount of water used, osmotic energy can be up to two orders of magnitude greater than bending energy, [26]. In an attempt to reach a new equilibrium state, organic molecules are rapidly expelled from the inner compartment to the surrounding medium, leading to a volume decrease. To minimize E_b, shape transformation must take place. This can occur either *via* the **prolate** pathway (towards tubes) or the **oblate** pathway [33] (towards discs and stomatocytes) (Figure 6).

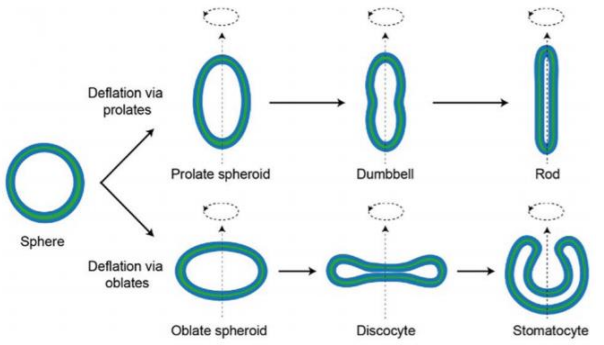

Fig. 6: The two different deflation routes – prolate and oblate – a polymersome can take when changing its shape. Adapted from [26]

This pathway commitment then depends on the parameter C_0: for $C_0 \geq 0$ shape transformation occurs through the prolate pathway; and conversely, the oblate one occurs when $C_0 < 0$, [17], [33], [34], [35].

The most systematic studies done on liposomes and lipidic vesicles have shed some light on the physicochemical origins of C_0 and computer simulations predicted that "By slightly changing the headgroup-headgroup and headgroup-water interaction of lipids in both monolayers separately, spontaneous curvature can be introduced in a membrane", [36]. C_0 was controllable and inducible through physicochemical anisotropy between the two leaflets of the bilayer membrane, [34].

It must be pointed out that C_0 is assumed to be laterally homogenous across the membrane and independent of the final shape, [37].

The following example illustrates the role of C_0 in shape transformation.

In a recent work, PEG−PDLLA polymersomes were induced into a shape transformation through the oblate pathway into stomatocytes, by generation of negative C_0 from transmembrane solvent anisotropy that forms during dialysis, [38]. They aimed to show that more relevant and biodegradable copolymers could be engineered into novel copolymeric architectures with desired shapes for nanomedical applications.

Internal and external solvent compositions are disproportional during dialysis and lead to different conformations of PEG chains. This is because chain expansion, quantified by the hydrodynamic chain volume (V_h), depends on solvent composition and the different solvation powers. This leads to an anisotropy between inner and outer membrane envelopes ($C_0 < 0$) that forces shape transformation (Figure 7).

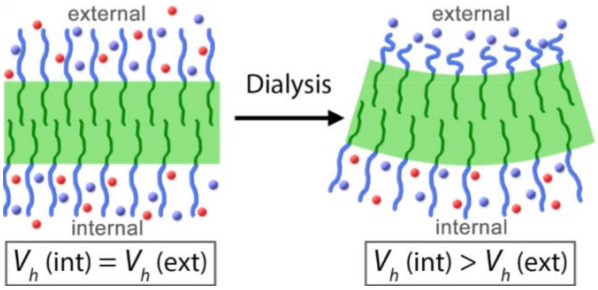

Fig. 7: During dialysis, the different solvent composition that arises on both sides of the membrane (internal and external), due to the semi-permeable membrane, makes external PEG chains partially collapse (in comparison to those on the interior) such that V_h (int) is greater than V_h (ext), inducing negative C_0 that directs shape transformation via the oblate pathway, toward stomatocytes. Adapted from [38]

4.1.2 Solvent Addition and Reverse Dialysis

Other mild methodologies for shape change are reported recently, [30]. They aim to control the shape transformation of the polymersomes into stomatocytes in a way that it becomes possible to encapsulate enzymes inside the stomach while not being harmed by the methodology.

For that, they start by forming polymersomes by the usual procedure: the addition of water to a

solution of polymer (PEG-*b*-PS) in THF/dioxane (4:1, v:v). The solvent is then removed by dialysis against water for at least 24 hours yielding polymersomes with glassy membranes.

Then, stomatocytes are either formed by the solvent addition method or by reverse dialysis of polymersomes.

(i) Solvent addition

Organic solvents are added *via* a syringe pump to the polymersome suspension. The polymersomes rapidly change into stomatocytes, which in turn gradually decrease their opening size with the increase of organic solvent, until a state of equilibrium of the osmotic pressure over the membrane is reached and the original polymersome spherical shape is obtained (Figure 8).

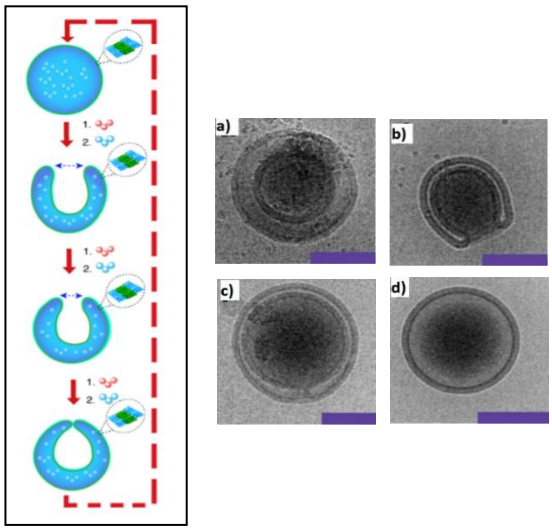

Fig. 8: The scheme on the left illustrates the reshaping process that occurs through the solvent addition methodology. (a) Transformation into stomatocytes with a large opening quickly occurs after the addition of 150 µL to a 500 µL polymersome solution (10 mg mL^{-1}). (b) and (c) The size of the opening continuously decreases until the stomatocytes are nearly closed. (d) Recovery of the spherical polymersome. Scale bars of 200nm. Adapted from [30]

In this process, a mixture of THF: dioxane (4:1 v/v) was added *via* a syringe pump (300 µL/h rate) until 700 µL were delivered to the polymersome solution (500 µL, 10 mg mL-1).

This methodology presents obvious advantages since reduced amounts of solvent are used and exposure times are reduced (the hole shape transformation cycle took about 2:30h), preventing enzyme denaturation during encapsulation.

Any given structure can be captured by rapid quenching with water. Furthermore, once rigid, the present morphology can once again re-enter the transformation cycle by repeating the process described in Figure 8 (left).

(ii) Reverse dialysis

The flexibility of the polymersome membrane can be obtained by adding organic solvent and water *via* dialysis such that a change in shape into stomatocytes can happen.

A solution of PEG_{44}-b-PS_{167} polymersomes (700 µL) was dialyzed against 150 mL water (50% in volume) and a mixture of 120.0 mL THF and 30.0 mL dioxane (4:1, v/v)

Figure 9 shows the evolution of the shape transformation of polymersomes at the start of the dialysis process (0 min), into stomatocytes (90min) that gradually close their opening with longer dialysis times (180min).

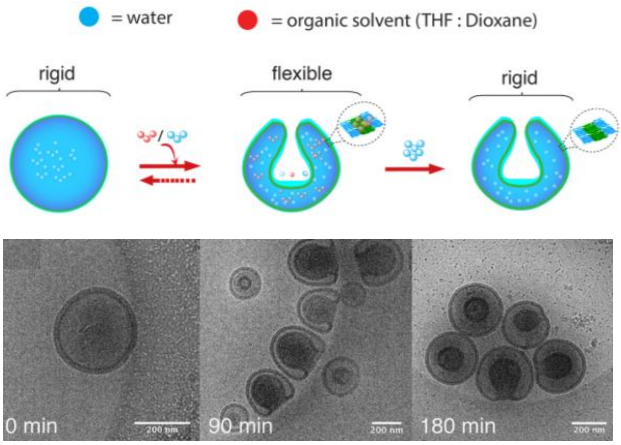

Fig. 9: Schematics of reverse dialysis of polymersomes (Top). Cryo-TEM images of polymersomes (0min) and stomatocytes (90 and 180min) were obtained after reverse dialysis in a mixture of water:THF:dioxane (1:0.8:0.2, v:v:v) (Bottom). Adapted from [30]

4.1.3 Salt Induced

Another osmotically induced way of shaping the vesicles is by generating osmotic pressure using salt solutions instead of solvents (Figure 10). This is ideal when dealing with biological compounds such as enzymes and trying to make the nanosystem more biocompatible, [29].

The polymersomes prepared by the traditional solvent exchange method [27] are dialysed against a salt solution (5, 10, 25, and 50mM NaCl) instead of pure water. They observe the formation of stomatocytes and the average opening size

decreasing with the increase in salt concentration (Figure 11).

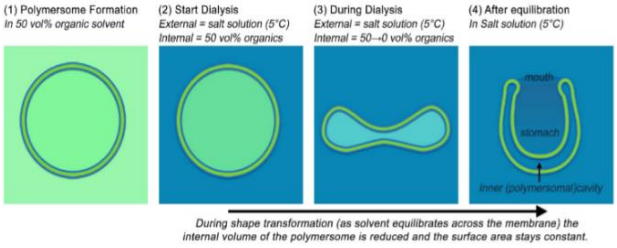

Fig. 10: Schematics of the shape transformation by dialysis against a salt solution

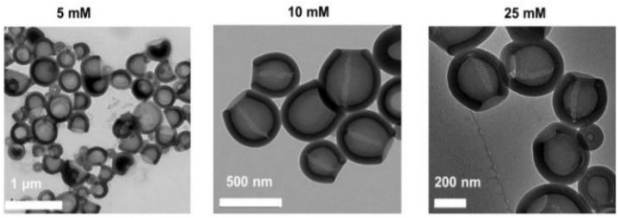

Fig. 11: TEM images of the resulting stomatocytes after dialysis against different salt concentrations. Adapted from [29]

Authors explain that salts can also induce controlled shape changes of polymersomes by influencing C_0, through polymer-ion or ion-hydrated polymer interactions [32] – based on the Hofmeister series, [39]. The study shows shape changes due to a variety of different salts and in different concentrations (Table 1).

Table 1. Shapes were obtained from variations of the cations at different concentrations. SV – spherical vesicle; ELL – ellipsoid; STO – stomatocyte; LCV – large compound vesicles. Adapted from [32]

conc. / shape / salt	1×10^{-2} M	1×10^{-3} M	1×10^{-4} M	1×10^{-5} M
NH_4Cl	STO	SV	SV	SV
NaCl	STO	SV&ELL	SV	SV
$MgCl_2$	LCV	STO	SV	SV
$CaCl_2$	LCV	STO	TUBE	ELL

Instead of dialysis, to the polymersome suspension (200µL), a total of 10µL of salt solution is directly added under a shaking speed of 1200 rpm. This is less time-consuming and yields a higher number of different controlled shapes.

4.2 Chemically Addition Strategy

Chemical addition can also be used to generate membrane anisotropy inducing shape transformation. Studies on liposomes already showed that by adjusting membrane composition, changes in shape could occur, [5], [6].

A concrete example of this approach used a cross-linker leading to a "cross-linker-induced shape transformation", [40]. This strategy achieves the change of polymersomes into tubes through a chemical stimulus. The block copolymers used – *poly(ethylene glycol)-block-poly(styrene-co-4-vinylbenzyl azide)* – contained side chains – *azide handles* – that allowed a reaction with a heterobifunctional crosslinker - *bicyclo[6.1.0]nonyne (BCN)*. Upon mixing, crosslinking takes place *via* a strain-promoted alkyne-azide cycloaddition (SPAAC) reaction. What is verified upon reaction is a sphere-to-tube transformation of previously prepared polymersomes occurring almost instantaneously.

They further demonstrate that the concentration of cross-linker (molar ratio of BCN/azide) plays a role in directing and extending the shape transformation, translating in longer tubes.

The shape transformation can be explained by the asymmetry generated by the difference in the number of azide handles in the outer polymersome membrane leaflet that react with the cross-linker, compared to the ones inside. This creates a positive C_0, leading to a shape change *via* the prolate pathway.

The authors also show the reversibility of the shape change process by cleaving a disulfide bridge of the utilized cross-linker, yielding the original polymersome vesicles. Another interesting, previously mentioned, resorts to azide groups to form hexagonally packed hollow hoops (HHHs), [29]. This process is schematically shown in Figure 12.

The morphology of polymersomes is not influenced by the azide groups in the absence of salt, but the transformation of polymersomes into HHHs is highly influenced by them when salt is present.

The group proposes that with the azide decoration of PEG, the anisotropy of the membrane is more enhanced by azide coordination with water molecules in the interior, which leads to an intensification of the effect that the organic solvent has on PEG in the inner compartment by solvation, thus increasing the hydrodynamic volume of the PEG chains at the internal side. A difference between the hydrodynamic volumes of the internal and external sides of the vesicles creates anisotropy, increasing the contribution of C_0 to the shape transformation process.

Fig. 12: Schematics of shape transformation of polymersomes either into stomatocytes or HHHs. Adapted from [29]

5 Shape Transformation Reversibility

For structures obtained from amphiphilic building blocks with a hydrophobic domain possessing a high glass transition temperature, reverting the shape should be possible by reverting the rigidifying process. In these cases, one must create a methodology to control the polymeric assemblies' glassy domain rigidity making it once again responsive and flexible to the environment.

Inspired by all the different shapes generated from liposomes, a controlled way to revert shape and search for different morphologies of polymeric vesicles is presented, [41]. Structures such as kippahs [42], oblates and polymersomes were obtained from stomatocytes (Figure 13).

To reshape the stomatocytes, the membrane had to recover its flexibility, mobility, and permeability. The originally used organic solvents (dioxane and THF) were re-used as good plasticizers of the PS hydrophobic domain in PEG_{44}-*b*-PS_{292}.

They found that quickly adding the solvents (50% of final solution) (THF:dioxane 75:25, v:v) to an aqueous stomatocytes solution, leads to structural disruption (Figure 14(i)). However, when the addition of the organic solvents to the aqueous solution of stomatocytes was gradually done by dialysis, different morphologies, corresponding to different ratios of THF:dioxane where obtained (Figure 14a, b, c and d).

Further experiments led the authors to conclude that the morphology present at the beginning of the shape transformation experiment highly influences the transformation process and the resultant morphologies.

In the study corresponding to Figure 8, the reversibility of the shape transformation is shown and even proposed to work cyclically.

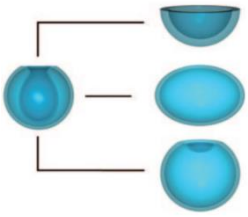

Fig. 13: The transformation of stomatocytes into (from top to bottom): kippahs, oblates, and polymersomes. Adapted from [41]

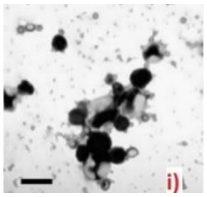

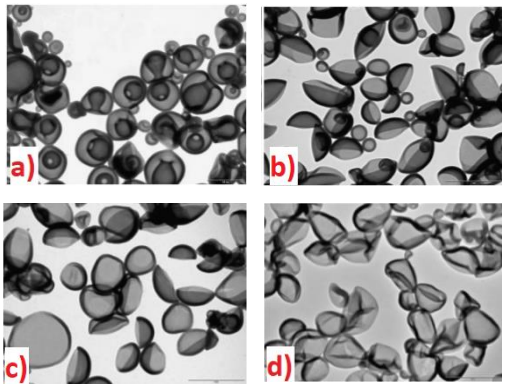

Fig. 14: (i) Quick addition of organic solvents leads to gross structural disruption and formation of polymer aggregates. (a) TEM image of the initial stomatocytes. (b) Kippahs resulting from dialysis of stomatocytes against THF:dioxane (75:25, v:v). (c) Oblates resulting from dialysis of stomatocytes against THF:dioxane (50:50, v:v). (d) Polymersomes resulting from dialysis of stomatocytes against THF:dioxane (25:75, v:v). Scale bar: 500nm. Adapted from supplementary information of [41]

6 Particle Characterization

As previously shown, non-spherical polymersome morphologies are kinetically trapped and analyzed by different characterization techniques.

Microscopy, generally in the form of Scanning Electron Microscopy (SEM) [43], Transmission Electron Microscopy (TEM), Cryo-TEM [44], is used to rapidly have an initial insight into the particle's shape, internal architecture, surface topography, morphology and also composition (Figure 15). Cryo-TEM is the most valuable tool as the samples are in a frozen-hydrated state instead of a dry-state.

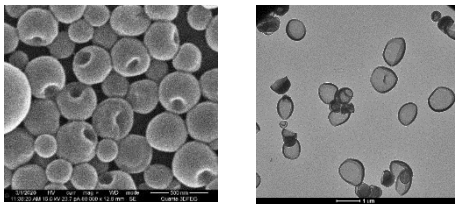

Fig. 15: SEM and TEM images of the resulting morphology of polymersomes dialyzed against 100mM NaCl and 50mM NaCl, respectively

Additional techniques are extensively used such as Dynamic Light Scattering (DLS), Magnetic Birefringence (MB) [45] (Figure 16), Zeta-potential, and Confocal microscopy, where the particles need to be fluorescently labeled, but can be visualized in the native solution state. Newer techniques such as liquid cell transmission electron microscopy (LC-TEM)[46] and super-resolution fluorescence microscopy techniques [47] are also available.

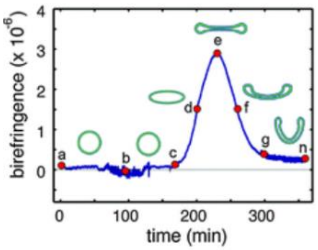

Fig. 16: Magnetic birefringence during dialysis of polymersomes at 2T. When the polymersomes start to deflate and become anisotropically shaped, there is an increase in the birefringence. Birefringence decreases when there is a partial inflation of stomatocytes. Adapted from [45]

7 Stomatocytes

As already mentioned above, stomatocytes are an interesting morphology obtained through the oblate pathway of transformation of polymersomes and present themselves as great structures for nanoreactors.

Stomatocytes are vesicles in the shape of a bowl with a "mouth" that opens for a cavity, the stomach (Figure 17).

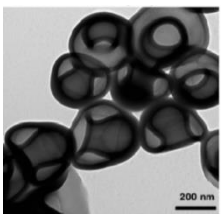

Fig. 17: Cryo-TEM images of PEG45-b-PS230 stomatocytes. Adapted from [27]

Reports show stomatocytes stay stable and preserve their morphology for months, making them future products "off-the-shelf", even when submitted to harsh physical conditions, such as high temperatures (70º, 1h) and ultra-sonication (45 kHz, 200 W, 5 min at 50 °C), [27].

Controlling the size of the stomatocytes and the size of the opening of the stomatocytes:

Different organic solvents utilized to dissolve the polymers and to prepare stomatocytes render different sizes of the resulting particles. The organic solvents should be chosen according to the block copolymers used.

Particles with a desired size can be obtained by successive passing of the particle suspension, under high pressure, through filters with desired pore sizes. Reports show the attempt to use an electrical field (AC) to prepare Ps with a narrow size distribution, [21], [48].

The opening of stomatocytes gradually decreases its size as the shape change process progresses, until equilibrium is reached [27] (Figure 3). They further found that the ratio of the organic solvents used also influences the final opening size. THF and dioxane are initially used in a 1:1 volume ratio, but later THF content in the mixture is increased to 65%, but at a fixed 50% vol. of water (organic solvents: water, 50:50, v:v). They also observed an almost linear relationship between the amount of THF present and the size of the stomatocyte's opening (Figure 18). As THF(%) increases, a/b decreases.

The same relationship is observed if the percentage of water in the final mixture is different from the original 50% while fixing the organic mixture on a 1:1 ratio. A reduced water content induces a longer shape change process since the rate of kinetic vitrification is slowed down, generating stomatocytes with narrower openings (smaller diameters).

The solvent mixture that is utilized to dissolve the polymer can, by itself, change the outward diffusion rate of organic solvent, upon dialysis, leading to different results. Previous observations show that a higher degree of swelling of the membrane occurs with THF in comparison to dioxane[49]. This means that the membrane's flexibility is preserved over longer periods if higher percentages of THF are used, resulting in a possible decrease in the size of the opening of stomatocytes. Using shorter hydrophobic polymeric domains will also keep the membrane more fluidic and flexible, contributing to the same effect, [27].

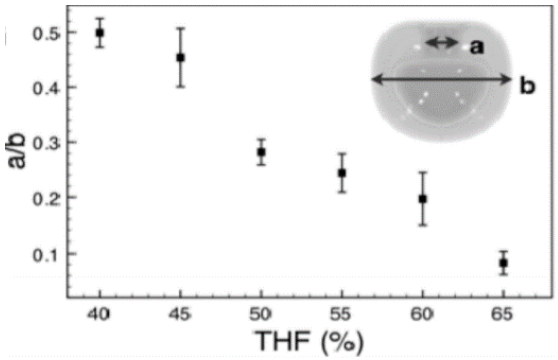

Fig. 18: The size of the stomatocyte's opening according to THF percentage in the solvent mixture with a fixed 50% vol. of water. Adapted from [27]

Another report shows the control over the opening of stomatocytes, made from diamagnetic amphiphilic block-copolymers with a highly anisotropic magnetic susceptibility, using magnetic fields with different strengths, [50]. The non-invasive nature of these applications using magnetic fields as external stimuli is of great interest in the medical field, [51], [52], [53], [54], [55].

The existence of a compartment with an opening that can be adjusted makes stomatocytes an interesting nanocontainer, accessible for surrounding molecules or catalytic species. The controllable different morphologies and structural robustness of the particles can contribute to novel applications in different fields.

7.1 Stomatocytes as Nanoreactors and Drug Delivery Systems

Polymeric assemblies are very versatile in shape. The shape of a particle greatly influences cellular uptake and immune regulation, [8].

By acting as a drug carrier, the polymeric vesicle must be able to reach the site of interest and, once there, release the cargo in a controlled manner.

Polymersome stomatocytes are a safe environment to carry the cargo because they protect it from the exterior. Hydrophilic or hydrophobic drugs can both be loaded.

In the case of nanoreactors, as seen in nature, shielding the enzymes within a bounded structure protects them from degradation and other harmful environmental factors, letting them carry out their normal catalytic activities for longer periods. The architecture of stomatocytes allows the enzymes to still be able to interact with external matter such as the substrate, something similar to what happens in biological systems.

Since stomatocytes allow for a high local concentration of catalyst and easy access of the substrate to the cavity, they are a very appealing tool in catalytic aqueous processes, [56].

Furthermore, multi-compartmentalization will enable multiple processes to occur close to each other, without interfering or inter-degrading. This architecture will evolve artificial organelles and nanoreactors as they will resemble more the biological scenario.

7.1.1 Stomatocytes for Drug Delivery / Nanocarriers

In drug delivery or controlled cargo release, the creation of responsive and "intelligent" vesicles is of interest. These structures respond to physical stimuli such as pressure, temperature, magnetic fields, ultrasound, and light, and to chemical stimuli such as changes in pH, glucose, enzymes, or response to ROS, [57], [58].

Designing the nanocontainer implies knowing which environment it will face within the organism. For example, we know the pH of the gastrointestinal tract of a human changes along its length (pH 2 in the stomach, pH 5-8 in the intestine), [59]. The cancerous environment is mainly acidic (pH 6.5-7.2), endosomes (pH 5.0,6.5), and lysosomes (pH 4.5-5). Smart polymersomes specifically stomatocytes can respond to external stimuli and be categorized as pH-responsive, light-responsive, thermosensitive, redox conditions responsive, magnetic field sensitive, and responsive to ionic strength and concentration of glucose.

pH-responsive polymers have titratable functionalities in the pendant groups or in the polymer backbone that can be ionized or deionized as a result of the change in pH, depending on their pKa. This, in turn, affects the hydrophilic/hydrophobic behavior of the polymersome membrane leading to different outcomes. Different morphologies have been obtained to date by going from low to high pH or reversely, [60], [61], [62].

In the case of thermosensitive polymers, the changes in temperature lead either to the formation of stomatocytes, disintegration, or opening through spontaneous membrane inversion or rearrangement, [63], [64].

In response to the stimuli, the particles can briefly have three responses that lead to a release of the cargo: a) disassembly / total disruption; b) change in membrane permeability, leading to a controlled and slower release; c) change in morphology (for example opening of the neck).

Especially in b), the size of the nanocontainers can affect the rate of cargo release, since the diffusion across the membrane, due to a gradient difference of the molecules between the interior and exterior depends on the membrane thicknes, s[65]. Ideally, through the design of the block copolymers and control over the conditions of preparation of the particles, one would be able to choose and dictate the rate of release of the cargo, [66].

Several initial studies successfully stably integrated different compounds in polymersomes, [67], [68].

The premise that polymeric vesicles and its membrane can change as a response to different stimuli, starts the path to building controlled delivery systems, [60], [61], [69], [70].

The encapsulation efficiency and the drug loading capacity are important for a system to be clinically and industrially relevant, since, if needed to attain the therapeutic window, one needs to inject higher quantities of nanoparticles. The drug molecules can be incorporated by dissolving them with the block copolymers, in an organic solvent suited for both the cargo and the membrane-forming building blocks, and then starting the self-assembly process.

In general, PEGylation can render nanocarriers more stealthy inside the organism and prolong their circulation while avoiding phagocytosis, [71].

A possible candidate for an anticancer drug delivery system was shown in [72], where platinum-loaded hybrid stomatocytes (both PEG-*b*-PCL [73], [74] and PEG-*b*-PS) nanomotors are self-assembled. One of the advantages of this system is that it is self-propelled, meaning it can penetrate tissues and cellular barriers [75], [76] and follow gradients of its fuel, in this case hydrogen peroxide [77].

The building blocks of the particles were PEG-*b*-PCL mixed with PEG-*b*-PS at different ratios of weight/weight (0/100, 25/75, 50/50, 75/25, and 100/0, respectively). By the traditional methodology[27] stomatocytes were formed when PEG-*b*-PCL was less than 75% in the mixture. The hydrophilic drug Dox was loaded in the water lumen when self-assembly took place. The incubation of stomatocytes with 50% PCL, loaded with this drug, with citric acid/Na_2HPO_4 buffer (pH=1), produced a decrease in the pH, resulting in the formation of large pores in the membrane and even full stomatocyte degradation, leading to a controlled drug release (Figure 19).

Additionally, both normal stomatocyte nanomotors (only PEG-*b*-PS) and hybrid stomatocyte nanomotors (PEG-*b*-PCL mixed with PEG-*b*-PS) were taken up by HeLa cells. In the case of the biodegradable hybrid stomatocyte nanomotor, observed by fluorescence analysis, the drug was diffused over the cell, which indicates drug release upon degradation. This was different from the dot-like fluorescence signal of the normal stomatocytes, meaning no or little drug release (Figure 20).

Indeed, the motion of the nanoscale motors directly facilitates the uptake by target cells since the movement increases the probability that contact between the target cells and the delivery system takes place.

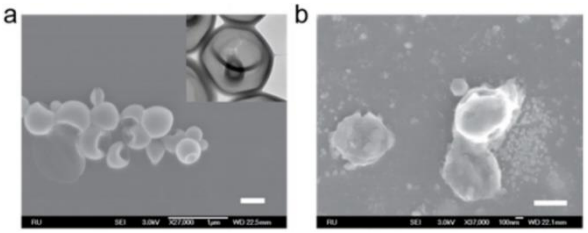

Fig. 19: SEM images of stomatocytes with 50% PEG-*b*-PCL before acidic degradation (a), and after acidic degradation (b). Scale bars of 400nm. Adapted from [72]

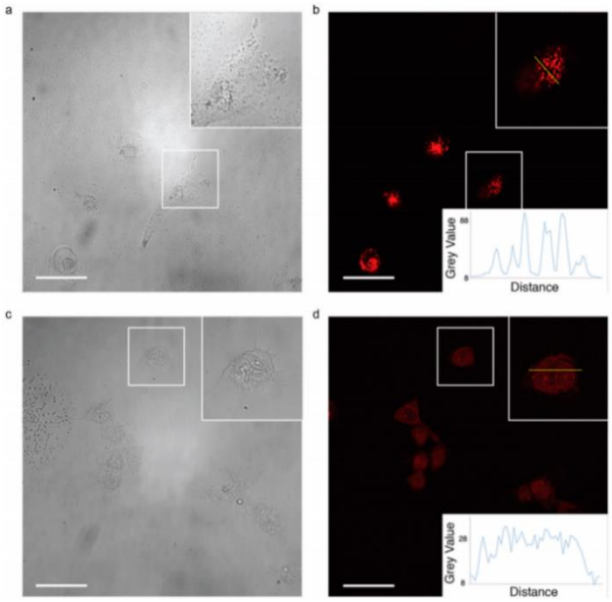

Fig. 20: (a) Bright-field images of cells after being incubated with normal stomatocytes in hydrogen peroxide. (b) Confocal images of cells after exposure to normal Dox-loaded stomatocytes. (c) Bright-field images of cells after being incubated with hybrid stomatocytes in hydrogen peroxide. (d) Confocal images of cells after exposure to hybrid Dox-loaded stomatocytes. Adapted from [72]

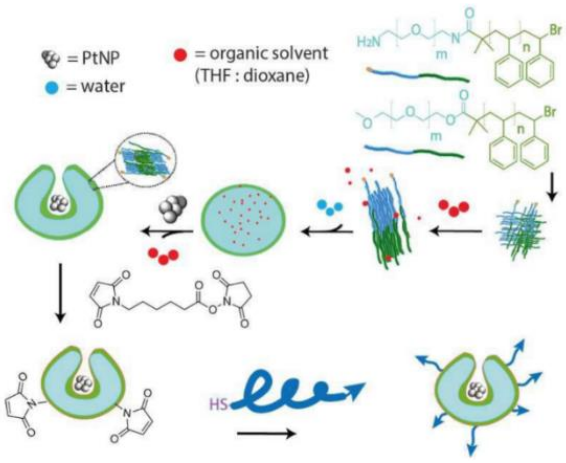

Fig. 21: Scheme illustrating the process of synthesis of tat functionalized stomatocyte nanomotors. Adapted from [76]

Another study shows the first functionalization of drug-loaded stomatocyte nanomotors with a cell-penetrating peptide (Figure 21), [76]. Trans-activator of transcription (tat) peptide, derived from the tat protein of HIV is used to functionalize the stomatocytes since it normally plays an important role in the entrance of the virus and cargo translocation to the cell interior, [78], [79].

Amine functionalized PEG_{66}-*b*-PS_{190} is utilized in 1% or 5% mixed with PEG_{44}-*b*-PS_{190} since the amine groups allow easy functionalization and modification with peptides (Figure 22).

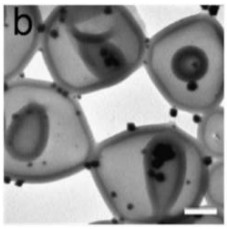

Fig. 22: TEM images of 5% FITC-tat functionalized stomatocyte nanomotors. Scale bar of 100nm. Adapted from [76]

Fluorescein isothiocyanate, FITC, is used as a model drug, facilitating the visualization in cell uptake experiments by confocal fluorescent microscopy.

HeLa cells are used to investigate the ability of the nanomotors to penetrate the cell. Both FITC PEGPS Pt stomatocytes and FITC-tat PEGPS Pt stomatocytes were incubated with the cells in a hydrogen peroxide solution. FITC-tat PEGPS Pt stomatocyte nanomotors were indeed taken up by the cells which remained intact. Some particles were also found still attached to the membrane, representing the beginning of internalization (Figure 23).

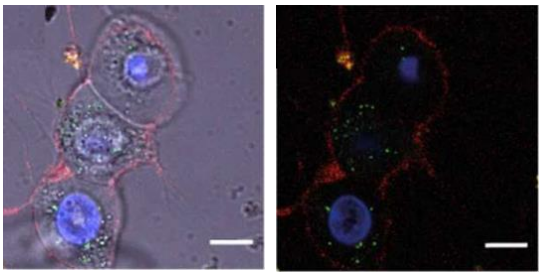

Fig. 23: Resulting in merged images of tat functionalized stomatocyte nanomotors in the presence of 0.015% hydrogen peroxide for 6 hours. Cell membrane stained in red (cell mask deep red). Nuclei stained in blue (live cell nucleus dye Hoechst 33342). Scale bars 10 μm. Adapted from [76]

Functionalized stomatocytes, FITC-tat PEGPS Pt, showed a higher ability of cell penetration compared to FITC PEGPS Pt stomatocytes. Furthermore, increased penetrating abilities were observed when, in the presence of hydrogen peroxide, the stomatocytes revealed an autonomous movement.

Although they use a non-biodegradable PEG-PS copolymer, this is an initial report representing the many possibilities in the design of nanodevices for drug delivery.

Conjugation of targeting molecules or moieties onto the stomatocyte's membrane can be done by conjugating the molecule to active groups present in the membrane after the vesicle is already formed or by conjugating the targeting ligand to the amphiphilic blocks before the stomatocyte formation. Click chemistry is being intensively used to achieve high degrees of surface functionalization through click reactions, [80], [81].

7.1.2 Stomatocytes as Nanoreactors

Such as enzymes, and biocatalysts are molecules capable of converting substrates selectively and efficiently. They are very sensitive to all the factors around them and can easily be deactivated in the presence of nullifying molecules, such as proteases, and harsh ambient conditions. Biocatalysts are better than traditional methods to speed up chemical reactions because the process involves mild reaction conditions (temperature, pressure, and pH), generally comprises fewer steps, is less expensive, avoids the use of environmentally undesired organic solvents and generates less waste.

The pool of available enzymes is constantly expanding thanks to DNA recombinant techniques and with the advance of science and technology, we can now create and arrange enzymes with improved

properties for desired applications. Creating micro/nanoreactors able to intracellularly compensate and rectify for the lost or decreased cellular function is an area of high importance in health investigation since these nanoreactors could be a good new solution in the context of enzyme replacement therapy.

Shape transformation of polymersomes into stomatocytes involves the use of significant amounts of organic solvents[27]. However, it was observed that they are often not compatible with the entrapment of proteins and enzymes because they cause denaturation.

Novel methodologies need to be implemented so that biomolecules can be encapsulated in different polymersome morphologies.

Encapsulation in stomatocytes

Enzyme immobilization is useful, since the handling of the enzymes, the separation of the product, and the recovery and re-usage are easier. It also renders enzymes more stable, less susceptible to changes in pH and temperature, and more resistant to denaturation.

There are three main traditional methods for immobilization: binding to a carrier (in a physical, ionic, or covalent way), encapsulation/entrapment (inclusion of the enzyme in a network), and cross-linking.

As previously described, the mild methodology reported recently, for stomatocyte preparation, was developed to entrap enzymes inside the stomach, while not being harmed by the methodology[30].

The normal procedure of preparing polymersomes is done by adding water to a solution of copolymers (PEG-*b*-PS) in THF/dioxane (4:1, v:v). The solvent is then removed by dialysis against water for at least 24 hours yielding polymersomes with glassy membranes.

Through the solvent addition method, stomatocytes are prepared using low amounts of solvent (Figure 8). Enzyme encapsulation is done by adding the optimal quantity of enzymes to an aqueous suspension of stomatocytes previously prepared through a mild solvent addition method and left stirring for at least 30 minutes. By then adding solvent, and returning to the cycle of shape transformation, the opening of the stomatocytes is gradually closed so that the enzymes are retained in the inner cavity (the hydrodynamic diameter of the enzymes one wants to load needs to be considered so that the opening size is controlled accordingly) (Figure 24). Afterwards, the removal of the non-encapsulated enzymes and the organic solvent is done by spin filtration and dialysis against a salt solution of 5mM $NaNo_3$. Control over the closure of the neck of the stomatocytes (the process needed to entrap the enzymes) is done by simply adding 150 μL of organic solvent to a 500 μL polymersome suspension within only 30 min.

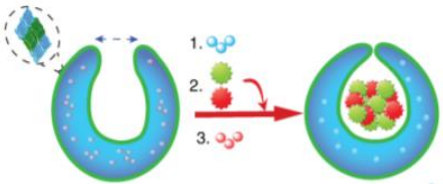

Fig. 24: Schematics of the process of enzyme entrapment by use of low amounts of organic solvent. 1. Water 2. Enzymes 3. Organic solvent. Adapted from [30]

The methodology presents obvious advantages, as already mentioned above, using smaller amounts of solvent with fewer exposure periods, aiming to preserve enzyme activity. Furthermore, the shape transformation cycle they propose includes the structures for both enzyme entrapment and cargo release.

More recently, milder cross-linking conditions of enzyme nano aggregates inside the cavity of PEG-PS stomatocytes enable to better preserve the enzyme activity in comparison to macroscopic CLEA processes, [56] (Figure 25).

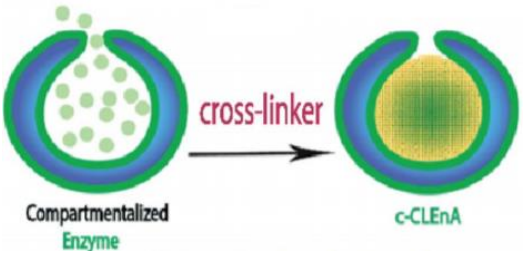

Fig. 25: Development of compartmentalized-cross-linked enzyme nano-aggregates (c-CLEnA) inside the stomatocytes *via* cross-linker addition. Adapted from [56]

CLEAs, a process of immobilization of enzymes through cross-linking of enzyme aggregates, offer the scenario where there is a highly concentrated stable enzyme activity with low production costs when compared to CLECs – cross-linked enzyme crystals and free-enzyme solution.

The aggregates are prepared by precipitation of the enzymes in an aqueous solution, by the addition of either organic solvents, salts, or non-ionic polymers. The tertiary structure of the aggregates is kept because non-covalent bonds hold them together. The aggregates become permanently

insoluble, and their superstructure and catalytic activity are preserved upon cross-linking.

Glutaraldehyde is often used as the cross-linking agent since it is low-priced and easily available in significant quantities. It was however verified that this agent didn't work with some enzymes as there was a small or no retention of activity.

The initial encapsulation of the enzyme of interest (PLE - porcine liver esterase and CalB - Candida antarctica Lipase B) was performed using the same method, [30]. Using previously prepared open-neck stomatocytes, the enzyme is encapsulated by narrowing the neck through the addition of organic solvent which is later removed. Encapsulation efficiency was reported to be ranging from 8% to 35%, depending on the initial feed of enzymes and their properties.

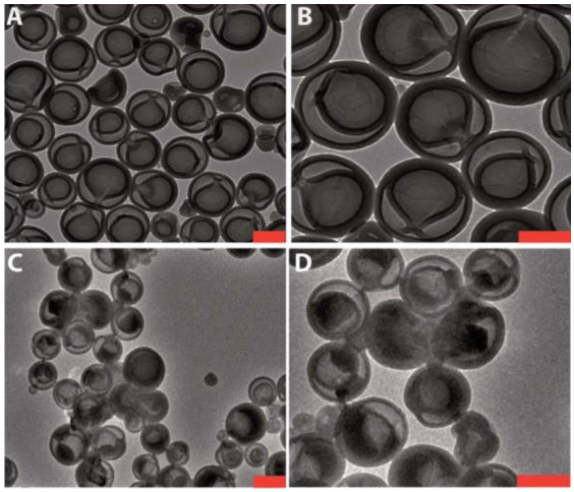

Fig. 26: PEG-PS stomatocytes loaded with CalB (Candida antarctica Lipase B) enzyme (A and B). CalB c-CLEnAs – cross-linked CalB compartmentalized inside the stomach (C and D). Scale bars 200nm. Adapted from [56]

Authors used both glutaraldehyde (control) and genipin [82] as cross-linking agents. The cross-linking of the aggregates is done inside the stomach, which is the template, yielding nano aggregates with more controlled sizes (Figure 26).

For both genipin and glutaraldehyde, the cross-linking process inside the stomatocytes was shown to be more efficient than the cross-linking of a free enzyme solution at the same concentrations.

To prove the ability to act as a catalytic system, activity tests and characterization of the particles were made in the c-CLEnAs unloaded from the stomatocytes, by adding an excess of organic solvent (Figure 27).

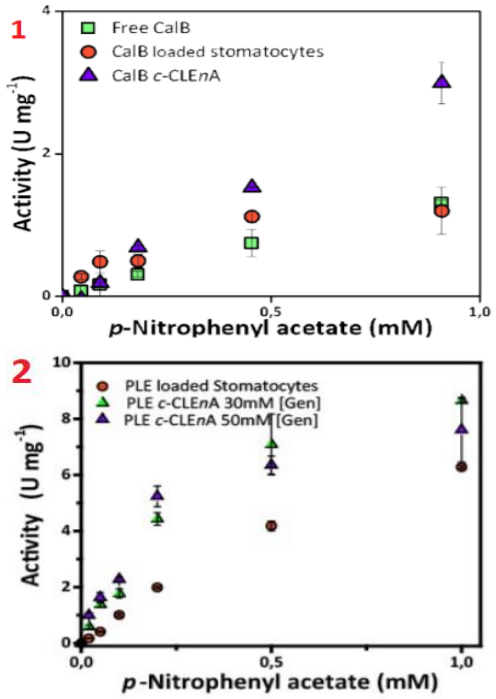

Fig. 27: (1) Comparison of specific activity (U mg^{-1}) in CalB-mediated hydrolysis of p-nitrophenyl acetate (pNPA) between the free enzyme, CalB loaded stomatocytes (with-out cross-linking) and CalB c-CLEnA. (2) Comparison of specific activity (U mg^{-1}) in PLE (porcine liver esterase)-mediated hydrolysis of p-nitrophenyl acetate (pNPA) between PLE loaded stomatocytes (without cross-linking) and PLE c-CLEnAs prepared with different concentrations of genipin. Adapted from the supporting information of [56]

The study highlights why stomatocytes are an interesting tool in catalytic processes through the effect of enzyme compartmentalization: increased enzyme local concentration, easy access to the substrate, and facilitated cross-linking process. They further show that the structures (c-CLEnAs) can be re-used in flow applications (Figure 28) over the course of at least 5 runs (Figure 29) with no loss in activity and no significant leaching when compared to CalB loaded stomatocytes with no cross-linked enzyme.

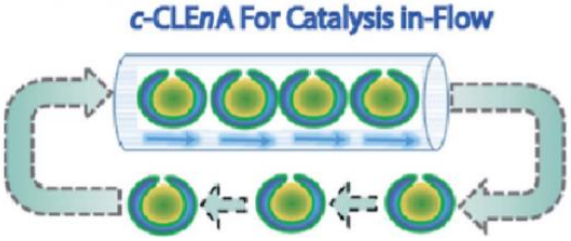

Fig. 28: c-CLEnA application and reusage for in-flow catalysis. Adapted from [56]

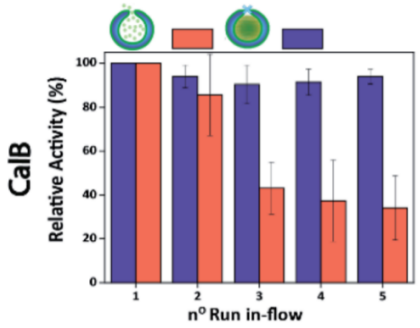

Fig. 29: Comparison between the relative activity of (red) CalB loaded stomatocytes and (blue) CalB c-CLEnAs (both with 33% encapsulation efficiency) over the course of five runs. Adapted from [56]

8 Conclusion

In this document, an overview of polymersome preparation and shape transformation methods was presented.

Stomatocytes are indeed supramolecular assemblies with very interesting structural characteristics and possess the advantages of polymeric vesicles. Methodologies to prepare these structures are evolving every day, searching for a standardized and simple producing process contributing to affordable "off the shelf" applications in nanomedicine and other areas.

Studies related to the interaction between these particles and cells and with the whole living system are still necessary to better understand the cross-talk that happens at a molecular level and what influences the particle has on the host. Mechanisms of endocytosis of stomatocytes and other polymeric vesicles need to be understood for better design of the particles to fulfill the desired purposes[83]. It is possible to manipulate the endocytosis mechanism through the size, shape, surface composition, and topology of the nanoparticle. For stable introduction of a nanoreactor inside the cell, the stomatocyte needs to be internalized while surviving the destructive reaction that cells might have. Functionalization with well-known moieties and target ligands will provide a way for targeted delivery. Stimuli responsiveness gives a lot of control over the particle's behavior inside the organism and inside the cells.

The full potential of these particles is not yet developed. It is expected that further work can create affordable drug delivery and stable bio-catalysis systems contributing to public health improvement and an environmental impact decrease.

References:

[1] G. Habermehland, A. Press, A. Haaf, G. Haaf, K. Oka, and Y. Shimizu, "A Totally Synthetic Bilayer Membrane," *Journal of the American Chemical Society*, vol 99, no.11, pp. 7–8, 1977, doi: 10.1021/ja00453a066.

[2] N. Grimaldi, F. Andrade, N. Segovia, L. Ferrer-Tasies, S. Sala, J. Veciana, and N. Ventosa., "Lipid-based nanovesicles for nanomedicine," *Chemical Society Reviews*, vol. 45, no. 23, pp. 6520–6545, 2016, doi: 10.1039/c6cs00409a.

[3] T. Einfalt, D. Witzigmann, C. Edlinger, S. Sieber, R. Goers, A. Najer, M. Spulber, O. Onaca-Fischer, J.Huwyler, and C. G. Palivan "Biomimetic artificial organelles with in vitro and in vivo activity triggered by reduction in microenvironment," *Nature Communications*, vol. 9, no. 1, pp. 1–12, 2018, doi: 10.1038/s41467-018-03560-x.

[4] C. Xu, S. Hu, and X. Chen, "Artificial cells: from basic science to applications," *Materials Today*, vol. 19, no. 9, pp. 516–532, 2016, doi: 10.1016/j.mattod.2016.02.020.

[5] H. Hotani, "Transformation pathways of liposomes," *Journal of Molecular Biology*, vol. 178, no. 1, pp. 113–120, 1984, doi: 10.1016/0022-2836(84)90234-1.

[6] R. Lipowsky, "The conformation of membranes," *Nature*, vol. 349, pp. 475–481, 1991.

[7] E. Rideau, R. Dimova, P. Schwille, F. R. Wurm, and K. Landfester, "Liposomes and polymersomes: a comparative review towards cell mimicking," *Chemical Society reviews*, vol. 47, no. 23, pp. 8572–8610, 2018, doi: 10.1039/c8cs00162f.

[8] D. E. Discher and F. Ahmed, "Polymersomes," *Annual Review of Biomedical Engineering*, vol. 8, no. 1, pp. 323–341, 2006, doi: 10.1146/annurev.bioeng.8.061505.095838.

[9] W. A. Braunecker and K. Matyjaszewski, "Controlled/living radical polymerization: Features, developments, and perspectives," *Progress in Polymer Science (Oxford)*, vol. 32, no. 1, pp. 93–146, 2007, doi: 10.1016/j.progpolymsci.2006.11.002.

[10] K. Matyjaszewski, "Atom Transfer Radical Polymerization (ATRP): Current status and future perspectives," *Macromolecules*, vol. 45, no. 10, pp. 4015–4039, 2012, doi: 10.1021/ma3001719.

[11] J. Chiefari, Y. K. Chong, F. Ercole, J. Krstina, J. Jeffrey, T. P. T. Le, R. Mayadunne, G. F. Meijs, C. L. Moad, G. Moad, E. Rizzardo, and S. H. Thang, "Living free-radical polymerization by reversible addition - Fragmentation chain transfer: The RAFT process," *Macromolecules*, vol. 31, no. 16, pp. 5559–5562, 1998, doi: 10.1021/ma9804951.

[12] V. Balasubramanian, B. Herranz-Blanco, P. V. Almeida, J. Hirvonen, and H. A. Santos, "Multifaceted polymersome platforms: Spanning from self-assembly to drug delivery and protocells," *Progress in Polymer Science*, vol. 60, pp. 51-85, 2016, doi: 10.1016/j.progpolymsci.2016.04.004.

[13] J. N. Israelachvili, D. J. Mitchell, and B. W. Ninham, "Theory of self-assembly of hydrocarbon amphiphiles into micelles and bilayers," *Journal of the Chemical Society, Faraday Transactions 2: Molecular and Chemical Physics*, vol. 72, pp. 1525–1568, 1976, doi: 10.1039/F29767201525.

[14] D. D. Lasic, "Novel applications of liposomes," *Trends in Biotechnology*, vol. 16, no. 7, pp. 307–321, 1998, doi: 10.1016/S0167-7799(98)01220-7.

[15] P. Fromherz, "Lipid-vesicle structure: Size control by edge-active agents," *Chemical Physics Letters*, vol. 94, no. 3, pp. 259–266, 1983, doi: 10.1016/0009-2614(83)87083-3.

[16] J. Habel, A. Ogbonna, N. Larsen, L. Schulte, K. Almdal, and C. Hélix-Nielsen, "How molecular internal-geometric parameters affect PB-PEO polymersome size in aqueous solution," *Journal of Polymer Science, Part B: Polymer Physics*, vol. 54, no. 7, pp. 699–708, 2016, doi: 10.1002/polb.23954.

[17] R. S. M. Rikken, H. Engelkamp, R. J. M. Nolte, J. C. Maan, J. C. M. van Hest, D. A. Wilson, and P. C. M. Christianen, "Shaping polymersomes into predictable morphologies via out-of-equilibrium self-assembly," *Nature Communications*, vol. 7, pp. 1–7, 2016, doi: 10.1038/ncomms12606.

[18] F. Meng, C. Hiemstra, G. H. M. Engbers, and J. Feijen, "Biodegradable polymersomes," *Macromolecules*, vol. 36, no. 9, pp. 3004–3006, 2003, doi: 10.1021/ma034040+.

[19] J. P. Reeves and R. M. Dowben, "Formation and properties of thin-walled phospholipid vesicles," *Journal of Cellular Physiology*, vol. 73, no. 1, pp. 49–60, 1969, doi: 10.1002/jcp.1040730108.

[20] K. Kita-Tokarczyk, J. Grumelard, T. Haefele, and W. Meier, "Block copolymer vesicles - Using concepts from polymer chemistry to mimic biomembranes," *Polymer*, vol. 46, no. 11, pp. 3540–3563, 2005, doi: 10.1016/j.polymer.2005.02.083.

[21] H. Lomas, M. Massignani, K. A. Abdullah, I. Canton, C. Lo Presti, S. MacNeil, J. Du, A. Blanazs, J. Madsen, S. P. Armes, A. L. Lewis, and G. Battaglia, "Non-cytotoxic polymer vesicles for rapid and efficient intracellular delivery," *Faraday Discussions*, vol. 139, pp. 143–159, 2008, doi: 10.1039/b717431d.

[22] Miglena I. Angelova and Dimiter S. Dimitrov, "Liposome Electro formation," *Faraday Discussions*, vol. 81, pp. 303–311, 1986.

[23] T. P. T. Dao, M. Fauquignon, F. Fernandes, E. Ibarboure, A. Vax, M. Prieto, and J. F. Le Meins, "Membrane properties of giant polymer and lipid vesicles obtained by electroformation and pva gel-assisted hydration methods," *Colloids and Surfaces A: Physicochemical and Engineering Aspects*, vol. 533, no. September, pp. 347–353, 2017, doi: 10.1016/j.colsurfa.2017.09.005.

[24] T. Köthe, S. Martin, G. Reich, and G. Fricker, "Dual asymmetric centrifugation as a novel method to prepare highly concentrated dispersions of PEG-b-PCL polymersomes as drug carriers," *International Journal of Pharmaceutics*, vol. 579, pp. 119087, 2020, doi: 10.1016/j.ijpharm.2020.119087.

[25] L. K. E. A. Abdelmohsen, D. S. Williams, J. Pille, S. G. Ozel, R. S. M. Rikken, D. A. Wilson, and J. C. M. van Hest, "Formation of Well-Defined, Functional Nanotubes via Osmotically Induced Shape Transformation of Biodegradable Polymersomes," *Journal of the American Chemical Society*, vol. 138, no. 30, pp. 9353–9356, 2016, doi: 10.1021/jacs.6b03984.

[26] C. K. Wong, M. H. Stenzel, and P. Thordarson, "Non-spherical polymersomes: Formation and characterization," *Chemical Society Reviews*, vol. 48, no. 15, pp. 4019–4035, 2019, doi: 10.1039/c8cs00856f.

[27] K. T. Kim, J. Zhu, S. A. Meeuwissen, J. J. L. M. Cornelissen, D. J. Pochan, R. J. M. Nolte, and J. C. M. van Hest, "Polymersome stomatocytes: Controlled shape

transformation in polymer vesicles," *Journal of the American Chemical Society*, vol. 132, no. 36, pp. 12522–12524, 2010, doi: 10.1021/ja104154t.

[28] J. Brandrup, E. . Immergut, and E. . Grulke, *Polymer Handbook. Fourth Edition*. 1999.

[29] H. Che, L. N. J. de Windt, J. Zhu, I. A. B. Pijpers, A. F. Mason, L. E. A. Abdelmohsen, and J. C. M. van Hest, "Pathway dependent shape-transformation of azide-decorated polymersomes," *Chemical Communications*, vol. 56, no. 14, pp. 2127–2130, 2020, doi: 10.1039/c9cc08944f.

[30] L. K. E. A. Abdelmohsen, M. Nijemeisland, G. M. Pawar, G. A. Janssen, R. J. M. Nolte, J. C. M van Hest, and D. A. Wilson, "Dynamic Loading and Unloading of Proteins in Polymeric Stomatocytes: Formation of an Enzyme-Loaded Supramolecular Nanomotor," *ACS Nano*, vol. 10, no. 2, pp. 2652–2660, 2016, doi: 10.1021/acsnano.5b07689.

[31] P. L. Soo and A. Eisenberg, "Preparation of Block Copolymer Vesicles in Solution," *Journal of Polymer Science, Part B: Polymer Physics*, vol. 42, no. 6, pp. 923–938, 2004, doi: 10.1002/polb.10739.

[32] Y. Men, W. Li, C. Lebleu, J. Sun, and D. A. Wilson, "Tailoring Polymersome Shape Using the Hofmeister Effect," *Biomacromolecules*, vol. 21, no. 1, pp. 89-94, 2019, doi: 10.1021/acs.biomac.9b00924.

[33] U. Seifert and K. Berndl, "Shape transformations of vesicles: Phase diagram for spontaneouscurvature and bilayer-coupling models," *Physical Review*, vol. 44, no. 2, pp. 1182–1202, 1991, doi: 10.1103/PhysRevA.44.1182.

[34] R. Lipowsky, "Spontaneous tubulation of membranes and vesicles reveals membrane tension generated by spontaneous curvature," *Faraday Discussions*, vol. 161, pp. 305–331, 2012, doi: 10.1039/c2fd20105d.

[35] M. Jarić, M., Seifert, U., Wintz, W., & Wortis, "Vesicular instabilities: The prolate-to-oblate transition and other shape instabilities of fluid bilayer membranes." *Physical Review E*, vol. 52, no. 6, pp. 6623-6634, 1995, doi: 10.1103/physreve.52.6623.

[36] A. J. Markvoort, R. A. Van Santen, and P. A. J. Hilbers, "Vesicle shapes from molecular dynamics simulations," *Journal of Physical Chemistry B*, vol. 110, no. 45, pp. 22780–22785, 2006, doi: 10.1021/jp064888a.

[37] U. Seifert and R. Lipowsky, "Morphology of Vesicles," vol. 1, pp. 403–463, 1995, doi: 10.1016/S1383-8121(06)80025-4.

[38] I. A. B. Pijpers, L. K. E. A. Abdelmohsen, D. S. Williams, and J. C. M. Van Hest, "Morphology under Control: Engineering Biodegradable Stomatocytes," *ACS Macro Letters*, vol. 6, no. 11, pp. 1217–1222, 2017, doi: 10.1021/acsmacrolett.7b00723.

[39] Y. Zhang and P. S. Cremer, "Interactions between macromolecules and ions: the Hofmeister series," *Current Opinion in Chemical Biology*, vol. 10, no. 6, pp. 658–663, 2006, doi: 10.1016/j.cbpa.2006.09.020.

[40] M. C. M. Van Oers, F. P. J. T. Rutjes, and J. C. M. Van Hest, "Tubular polymersomes: A cross-linker-induced shape transformation," *Journal of the American Chemical Society*, vol. 135, no. 44, pp. 16308–16311, 2013, doi: 10.1021/ja408754z.

[41] S. A. Meeuwissen, K. T. Kim, Y. Chen, D. J. Pochan, and J. C. M. Van Hest, "Controlled shape transformation of polymersome stomatocytes," *Angewandte Chemie - International Edition*, vol. 50, no. 31, pp. 7070–7073, 2011, doi: 10.1002/anie.201102167.

[42] T. Azzam and A. Eisenberg, "Fully collapsed (kippah) vesicles: Preparation and characterization," *Langmuir*, vol. 26, no. 13, pp. 10513–10523, 2010, doi: 10.1021/la1004837.

[43] S. B. K. Kalsoom Akhtar, Shahid Ali Khan and and A. M. Asiri, "Chapter 4: Scanning Electron Microscopy: Principle and Applications in Nanomaterials Characterization," *Handbook of Materials Characterization*. 2018, doi: 10.1007/978-3-319-92955-2_4.

[44] R. F. Thompson, M. Walker, C. A. Siebert, S. P. Muench, and N. A. Ranson, "An introduction to sample preparation and imaging by cryo-electron microscopy for structural biology," *Methods*, vol. 100, pp. 3–15, 2016, doi: 10.1016/j.ymeth.2016.02.017.

[45] R. S. M. Rikken, H. H. M. Kerkennar, R. J. M. Nolte, J. C. Maan, J. C. M. van Hest, P. C. M. Christianen, and D. A. Wilson, "Probing morphological changes in polymersomes with magnetic birefringence," *Chemical Communications*, vol. 50, no. 40, pp. 5394–5396, 2014, doi:

10.1039/c3cc47483f.

[46] A. Ianiro, H. Wu, M. M. J. van Rijt, M. P. Vena, A. D. A. Keizer, A. C. C. Esteves, R. Tuinier, H. Freidrich, N. A. J. M. Sommerdijk, and J. P. Patterson, "Liquid–liquid phase separation during amphiphilic self-assembly," *Nature Chemistry*, vol. 11, no. 4, pp. 320–328, 2019, doi: 10.1038/s41557-019-0210-4.

[47] B. Huang, H. Babcock, and X. Zhuang, "Breaking the diffraction barrier: Super-resolution imaging of cells," *Cell*, vol. 143, no. 7, pp. 1047–1058, 2010, doi: 10.1016/j.cell.2010.12.002.

[48] G. Battaglia and A. J. Ryan, "Bilayers and interdigitation in block copolymer vesicles," *Journal of the American Chemical Society*, vol. 127, no. 24, pp. 8757–8764, 2005, doi: 10.1021/ja050742y.

[49] Y. Yu and A. Eisenberg, "Control of morphology through polymer-solvent interactions in crew-cut aggregates of amphiphilic block copolymers," *Journal of the American Chemical Society*, vol. 119, no. 35, pp. 8383–8384, 1997, doi: 10.1021/ja9709740.

[50] P. G. Van Rhee, R. S. M. Rikken, L. K. E. A. Abdelmohsen, J. C. Maan, R. J. M. Nolte, J. C. M. van Hest, P. C. M. Christianen, and D. A. Wilson , "Polymersome magneto-valves for reversible capture and release of nanoparticles," *Nature Communications*, vol. 5, pp. 1–8, 2014, doi: 10.1038/ncomms6010.

[51] A. Morales-García, M. Elena Arroyo-De Dompablo, A. G. Rousse, P. Senguttuvan, J. M. Tarascon, and M. Rosa Palacín, "Combining experiments and computations to understand the intercalation potential and redox mechanism for A2Ti3O7 (A=Li, Na)," *Materials Research Society Symposium Proceedings*, Boston, Massachusetts, vol. 1740, no. 3, pp. 31–36, 2015, doi: 10.1557/opl.2015.282.

[52] P. Walde, "Building artificial cells and protocell models: Experimental approaches with lipid vesicles," *BioEssays*, vol. 32, no. 4, pp. 296–303, 2010, doi: 10.1002/bies.200900141.

[53] W. L. Chiang, C. J. Ke, Z. X. Liao, S. Y. Chen, F. R. Chen, C. Y. Tsai, Y. Xia, and H. W. Sung, "Pulsatile drug release from PLGA hollow microspheres by controlling the permeability of their walls with a magnetic field," *Small*, vol. 8, no. 23, pp. 3584–3588, 2012, doi: 10.1002/smll.201201743.

[54] C. R. Thomas, D. P. Ferris, J. H. Lee, E. Choi, M. H. Cho, E. S. Kim, J. F. Stoddart, J. S. Shin, J. Cheon, and J. I. Zink, "Noninvasive remote-controlled release of drug molecules in vitro using magnetic actuation of mechanized nanoparticles," *Journal of the American Chemical Society*, vol. 132, no. 31, pp. 10623–10625, 2010, doi: 10.1021/ja1022267.

[55] H. Oliveira, E. Pérez-Andrés, J. Thevenot, O. Sandre, E. Berra, and S. Lecommandoux, "Magnetic field triggered drug release from polymersomes for cancer therapeutics," *Journal of Controlled Release*, vol. 169, no. 3, pp. 165–170, 2013, doi: 10.1016/j.jconrel.2013.01.013.

[56] M. T. De Martino, F. Tonin, N. A. Yewdall, M. Abdelghani, D. S. Williams, U. Hanefeld, F. P. J. T. Rutjes, L. K. E. A. Abdelmohsen, and J. C. M. van Hest, "Compartmentalized cross-linked enzymatic nano -aggregates (c -CLE n A) for efficient in-flow biocatalysis," *Chemical Science*, vol. 11, no. 10, pp. 2765–2769, 2020, doi: 10.1039/c9sc05420k.

[57] X. Hu, Y. Zhang, Z. Xie, X. Jing, A. Bellotti, and Z. Gu, "Stimuli-Responsive Polymersomes for Biomedical Applications," *Biomacromolecules*, vol. 18, no. 3, pp. 649–673, 2017, doi: 10.1021/acs.biomac.6b01704.

[58] H. Che and J. C. M. Van Hest, "Stimuli-responsive polymersomes and nanoreactors," *Journal of Materials Chemistry B*, vol. 4, no. 27, pp. 4632–4647, 2016, doi: 10.1039/c6tb01163b.

[59] D. F. Evans, G. Pye, R. Bramley, A. G. Clark, T. J. Dyson,and J. D. Hardcastle, "Measurement of gastrointestinal pH profiles in normal ambulant human subjects," *Gut*, vol. 29, no. 8, pp. 1035-1041, 1988, doi: 10.1136/gut.29.8.1035.

[60] U. Borchert, U. Lipprandt, M. Bilang, A. Kimpfler, A. Rank, R. Peschka.Suss, R. Schubert, P. Lindner, and S. Forster, "pH-induced release from P2VP-PEO block copolymer vesicles," *Langmuir*, vol. 22, no. 13, pp. 5843–5847, 2006, doi: 10.1021/la060227t.

[61] J. Du and S. P. Armes, "pH-responsive vesicles based on a hydrolytically self-cross-linkable copolymer," *Journal of the*

American Chemical Society, vol. 127, no. 37, pp. 12800–12801, 2005, doi: 10.1021/ja054755n.

[62] J. Rodríguez-Hernández and S. Lecommandoux, "Reversible inside-out micellization of pH-responsive and water-soluble vesicles based on polypeptide diblock copolymers," *Journal of the American Chemical Society*, vol. 127, no. 7, pp. 2026-7, 2005, doi: 10.1021/ja043920g.

[63] A. S. Mathews, C. S. Ha, W. J. Cho, and I. Kim, "Drug delivery system based on covalently bonded poly[N-isopropylacrylamide- co-2-hydroxyethylacrylate]-based nanoparticle networks," *Drug Delivery*, vol. 13, no. 4, pp. 245–251, 2006, doi: 10.1080/10717540500313067.

[64] J. E. Chung, M. Yokoyama, M. Yamato, T. Aoyagi, Y. Sakurai, and T. Okano, "Thermo-responsive drug delivery from polymeric micelles constructed using block copolymers of poly(N-isopropylacrylamide) and poly(butylmethacrylate)," *Journal of Controlled Release*, vol. 62, no. 1-2, pp. 115–127, 1999, doi: 10.1016/S0168-3659(99)00029-2.

[65] J. Siepmann, N. Faisant, J. Akiki, J. Richard, and J. P. Benoit, "Effect of the size of biodegradable microparticles on drug release: Experiment and theory," *Journal of Controlled Release*, vol. 96, no. 1, pp. 123–134, 2004, doi: 10.1016/j.jconrel.2004.01.011.

[66] A. Mecke, C. Dittrich, and W. Meier, "Biomimetic membranes designed from amphiphilic block copolymers," *Soft Matter*, vol. 2, no. 9, pp. 751–759, 2006, doi: 10.1039/b605165k.

[67] F. Ahmed, R. I. Pakunlu, A. Brannan, F. Bates, T. Minko, and D. E. Discher, "Biodegradable polymersomes loaded with both paclitaxel and doxorubicin permeate and shrink tumors, inducing apoptosis in proportion to accumulated drug," *Journal of Controlled Release*, vol. 116, no. 2 spec. iss., pp. 150–158, 2006, doi: 10.1016/j.jconrel.2006.07.012.

[68] W. Chen, F. Meng, R. Cheng, and Z. Zhong, "pH-Sensitive degradable polymersomes for triggered release of anticancer drugs: A comparative study with micelles," *Journal of Controlled Release*, vol. 142, no. 1, pp. 40–46, 2010, doi: 10.1016/j.jconrel.2009.09.023.

[69] H. Che and J. Yuan, "CO2-responsive bowl-shaped polymersomes," *Macromolecular Research*, vol. 25, no. 6, pp. 635–639, 2017, doi: 10.1007/s13233-017-5133-6.

[70] C. Pietsch U. Mansfeld, C. Guerrero-Sanchez, S. Hoeppener, A. Vollrath, M. Wagner, R. Hoogenboom, S. Saubern, S. H. Thang, C. R. Becer, J. Chiefari, and U. S. Schubert, "Thermo-induced self-assembly of responsive poly(DMAEMA-b-DEGMA) block copolymers into multi- and unilamellar vesicles," *Macromolecules*, vol. 45, no. 23, pp. 9292–9302, 2012, doi: 10.1021/ma301867h.

[71] A. L. Klibanov, K. Maruyama, V. P. Torchilin, and L. Huang, "Amphipathic polyethyleneglycols effectively prolong the circulation time of liposomes," *FEBS Letters*, vol. 268, no. 1, pp. 235–237, 1990, doi: 10.1016/0014-5793(90)81016-H.

[72] Y. Tu, F. Peng, A. A. M. André, Y. Men, M. Srinivas, and D. A. Wilson, "Biodegradable Hybrid Stomatocyte Nanomotors for Drug Delivery," *ACS Nano*, vol. 11, no. 2, pp. 1957–1963, 2017, doi: 10.1021/acsnano.6b08079.

[73] Y. Lu and S. C. Chen, "Micro and nano-fabrication of biodegradable polymers for drug delivery," *Advanced Drug Delivery Reviews*, vol. 56, no. 11, pp. 1621–1633, 2004, doi: 10.1016/j.addr.2004.05.002.

[74] X. Shuai, H. Ai, N. Nasongkla, S. Kim, and J. Gao, "Micellar carriers based on block copolymers of poly(ε-caprolactone) and poly(ethylene glycol) for doxorubicin delivery," *Journal of Controlled Release*, vol. 98, no. 3, pp. 415–426, 2004, doi: 10.1016/j.jconrel.2004.06.003.

[75] W. Gao and J. Wang, "Synthetic micro/nanomotors in drug delivery," *Nanoscale*, vol. 6, no. 18, pp. 10486–10494, 2014, doi: 10.1039/c4nr03124e.

[76] F. Peng, Y. Tu, A. Adhikari, J. C. J. Hintzen, D. W. P. M. Löwik, and D. A. Wilson, "A peptide functionalized nanomotor as an efficient cell penetrating tool," *Chemical Communications*, vol. 53, no. 6, pp. 1088–1091, 2017, doi: 10.1039/c6cc09169e.

[77] D. A. Wilson, B. De Nijs, A. Van Blaaderen, R. J. M. Nolte, and J. C. M. Van Hest, "Fuel concentration dependent movement of supramolecular catalytic nanomotors," *Nanoscale*, vol. 5, no. 4, pp. 1315–1318, 2013, doi: 10.1039/c2nr32976j.

[78] E. Vives, J.- Richard, C. Rispal, and B. Lebleu, "TAT Peptide Internalization: Seeking the Mechanism of Entry," *Current Protein & Peptide Science*, vol. 4, no. 2, pp. 125–132, 2005, doi: 10.2174/1389203033487306.

[79] A. Mishra, C. H. Lai, N. W. Schmidt, V. Z. Sun, A. R. Rodriguez, R. Tong, L. Tang, J. Cheng, T. J. Deming, D. T. Kamei, and G. C. L. Wong, "Translocation of HIV TAT peptide and analogues induced by multiplexed membrane and cytoskeletal interactions," *Proceedings of the National Academy of Sciences of the United States of America*, vol. 108, no. 41, pp. 16883–16888, 2011, doi: 10.1073/pnas.1108795108.

[80] G. Yi, J. Son, J. Yoo, C. Park, and H. Koo, "Application of click chemistry in nanoparticle modification and its targeted delivery," *Biomaterials Research*, vol. 22, no. 1, pp. 1–8, 2018, doi: 10.1186/s40824-018-0123-0.

[81] J. Lu, M. Shi, and M. S. Shoichet, "Click chemistry functionalized polymeric nanoparticles target corneal epithelial cells through RGD-cell surface receptors," *Bioconjugate Chemistry*, vol. 20, no. 1, pp. 87–94, 2009, doi: 10.1021/bc8003167.

[82] S. H. Chiou, T. C. Hung, R. Giridhar, and W. T. Wu, "Immobilization of lipase to chitosan beads using a natural cross-linker," *Preparative Biochemistry and Biotechnology*, vol. 37, no. 3, pp. 265–275, 2007, doi: 10.1080/10826060701386752.

[83] T. Hyeon and V. Rotello, "Endocytosis at the nanoscale," *Chemical Society reviews*, vol. 41, no. 7, pp. 2545–2561, 2012, doi:10.1039/C2CS15309B.

Contribution of Individual Authors to the Creation of a Scientific Article (Ghostwriting Policy)

Both authors contributed to the writing and revision of the text.

Sources of Funding for Research Presented in a Scientific Article or Scientific Article Itself

No funding was received for conducting this study.

Conflict of Interest

The authors have no conflicts of interest to declare.